Low Probability of Interception of an Advanced Noise Radar Waveform with Linear-FM

This research considers an advanced pulse compression noise (APCN) radar waveform possessing salient features from linear-FM (LFM) and noise waveforms. A cross-correlation model considering several chirp waveform profiles is used to simulate the output of a passive electronic intelligence (ELINT) intercept-receiver. By doing so we are able to demonstrate the low probability of interception (LPI) characteristic of the APCN waveform for different κ values.

I. INTRODUCTION

The chirp waveform serves as a preferred radar waveform because the resultant time-bandwidth product is nonunity [1]. A large bandwidth β may be realized without having to transmit an extremely short pulse duration τ. The idea of realizing large bandwidths with even larger pulse durations results in a pulse compression gain defined by the time-bandwidth product.

When considering the threat of electronic warfare (EW), a passive electronic intelligence (ELINT) intercept-receiver will systematically vary its bandwidth and sweep time parameters until it positively correlates with the radar waveform thereby maximizing its receiver signal-to-noise ratio (SNR) [2–6]. This implies that when the right set of parameters is chosen, the ELINT receiver is said to be matched to the radar waveform. Consequently, the corresponding radar operational characteristics are considered deterministic, and the radar system is therefore compromised by the ELINT receiver.

The chirp waveform has uniform power envelope and finite bandwidth. Furthermore, the chirp waveform has a unique yet well-recognized spectral response. The matched filter that maximizes the system output is shown in Fig. 1 and can be determined in a systematic fashion. This, by definition, makes matched filter processing a deterministic process, and the ability to reverse-engineer the matched filter makes passive ELINT intercept-receivers a serious threat to active radar. Because the chirp radar waveform is well defined, it can be considered a poor low probability of interception (LPI) waveform and is therefore vulnerable to the intercept process described.

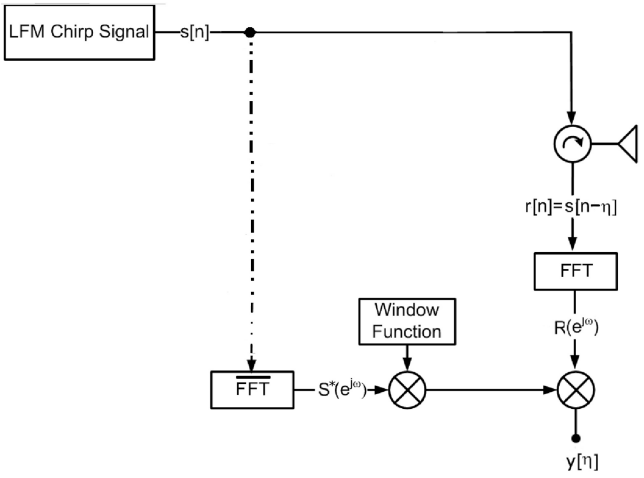

Fig. 1. Radar block diagram depicting matched filter receiver for chirp waveform.

An interest in using noise waveforms for radar-based applications has been pursued by several research groups [7–19]. The ideal noise waveform is random by nature, and is wide-sense stationary (WSS) as one would expect with a nondeterministic process. As a result interception becomes extremely difficult since each successive pulse or transmission is uncorrelated. Because of this the ideal noise waveform is considered a good LPI waveform [20–22].

The receiver for most noise radar systems is realized using a single-pass system where the signals are cross-correlated in the frequency domain. With a pulse compression system, a deramp on receive or "stretch" process ensures high sampling resolution over predetermined receive windows using a fairly simple receiver design. The stretch process greatly reduces the processing requirements of the system while providing high range-Doppler resolution inherent to the chirp waveform. This research identifies an advanced pulse compression noise radar waveform, abbreviated for simplicity as APCN, that adequately addresses the threat of interception without grossly impacting radar signal processing requirements or reducing radar target detection.

In this paper we demonstrate the vulnerability of chirp radar waveform by evaluating the output of a passive ELINT intercept-receiver. In doing so we provide justification as to why a secure pulse compression waveform is needed. In Section II we derive the signal basis for the APCN radar waveform and briefly discuss some of its characteristics. In Section III we evaluate the output of the intercept-receiver when cross-correlated with chirp and APCN ($0 \leq \kappa \leq 1$) waveforms. Lastly, conclusions on the work are presented in Section IV.

Manuscript received September 28, 2011; revised April 6 and July 12, 2012; released for publication October 31, 2012.

IEEE Log No. T-AES/49/2/944542.

Refereeing of this contribution was handled by R. Narayanan.

II. ADVANCED PULSE COMPRESSION NOISE RADAR WAVEFORM

The baseband, discrete-time equivalent of the complex chirp is defined as

$$s[n] = e^{j\pi\mu n^2} \qquad \text{for} \quad -N \le n \le N \tag{1}$$

where μ is the chirp rate, n is the discrete-time index, $T_s = \tau/N$ is the sampling period with pulse duration τ, and $s[n]$ is one of $N = 2^{\lceil \log_2(\tau\beta) \rceil}$ time samples. By discretizing the chirp and appreciating the fact that it has constant envelope with quadratic phase, we can represent (1) using vector notation as

$$\mathbf{s} = \begin{bmatrix} e^{j\pi\mu N^2} \\ e^{j\pi\mu(-N+1)^2} \\ \vdots \\ e^{j\pi\mu(N-1)^2} \\ e^{j\pi\mu N^2} \end{bmatrix}. \tag{2}$$

The noise waveform is also defined using vector notation, and has Rayleigh-distributed amplitude and uniformly-distributed phase. We represent the amplitude $\mathbf{a}$ and phase $\mathbf{p}$ of the advanced noise waveform (not pulse compressed) as

$$\mathbf{a} = \begin{bmatrix} a_{-N} \\ a_{-N+1} \\ \vdots \\ a_{N-1} \\ a_N \end{bmatrix}, \qquad \mathbf{p} = \begin{bmatrix} e^{j\kappa p_{-N}} \\ e^{j\kappa p_{-N+1}} \\ \vdots \\ e^{j\kappa p_{N-1}} \\ e^{j\kappa p_N} \end{bmatrix} \tag{3}$$

where κ is a phase scaling factor used to improve the contribution of the random phase component. If randomizing the phase is not essential, the scaling factor can be throttled to fully preserve the quadratic phase of the chirp component. The scaling factor is chosen from a set of values, $0 \le \kappa \le 1$.

By combining the chirp and noise waveforms, we can define the APCN waveform as

$$\mathbf{v} = \mathbf{a} \circ \mathbf{p} \circ \mathbf{s} = \begin{bmatrix} a_{-N} e^{j(\kappa p_{-N} + \pi\mu N^2)} \\ a_{-N+1} e^{j(\kappa p_{-N+1} + \pi\mu(-N+1)^2)} \\ \vdots \\ a_{N-1} e^{j(\kappa p_{N-1} + \pi\mu(N-1)^2)} \\ a_N e^{j(\kappa p_N + \pi\mu N^2)} \end{bmatrix} \tag{4}$$

where $(\circ)$ represents the Hadamard (element-wise) product. The discrete random values for the noise component of the APCN are predetermined in memory and are designed to vary at a rate equivalent to the fast-time digitization rate of the direct digital synthesizer (DDS). This rate is calculated as N/τ where N is the total discrete time samples used in realizing the uncompressed pulse duration τ. As each discrete frequency value for the linear-FM (LFM) component of the APCN is realized, a different random amplitude and phase value is also realized.

Next, we consider a point target of arbitrary reflectivity ζ whose radar cross section (RCS) is constant over time and frequency, and is moving with radial velocity v relative to the radar. The resultant delay $d = t_0 - (2v/c)t$ where t_0 is the target initial delay, v is the radial velocity, c is the speed of light, and t is continuous-time. After discretization of the receive signal, the target delay d will correspond to a discrete-time sample that will most likely not be an integer value. A quantizer implements the rounding operation, but in doing so, causes a range measurement error since the precision of the quantizer is limited. Therefore, the receive signal plus noise can be written as $x[n] = \zeta \cdot v[n-\eta] + \epsilon[n]$ where $\eta = d/T_s$ rounded to the nearest integer such that $\eta \in \mathcal{Z}[-N, N]$.

III. OUTPUT OF INTERCEPT-RECEIVER

To adequately demonstrate the vulnerability of the chirp radar waveform, several assumptions including the criterion for successful interception have been made about our intercept-receiver. They are as follows.

1) The intercept-receiver is passive by design, and therefore, does not transmit redirected energy as one expects with active jamming as considered in [12].

2) The sole intention of the receiver is to successfully intercept the radar waveform, and identify the operational characteristics such as pulse duration, bandwidth, and chirp rate.

3) The intercept-receiver has some general replica (not exact) of the chirp stored in memory, where the term "general replica" refers to the signal whose impulse response maximizes the intercept-receiver output when correlated with the radar waveform.

4) The intercept-receiver adjusts its impulse response by systematically varying bandwidth and sweep time parameters until correlation with the chirp is achieved.

5) Correlation is measured internally using a generic threshold detector. When the detection threshold is met or exceeded, the system is said to be matched and interception of the chirp waveform is achieved.

For the case of the sensed chirp waveform $g[n]$, the intercept-receiver has a library of M chirp replicas $\tilde{s}_M[n]$ stored in memory. The different instantiations are used in building the cross-correlation output of the

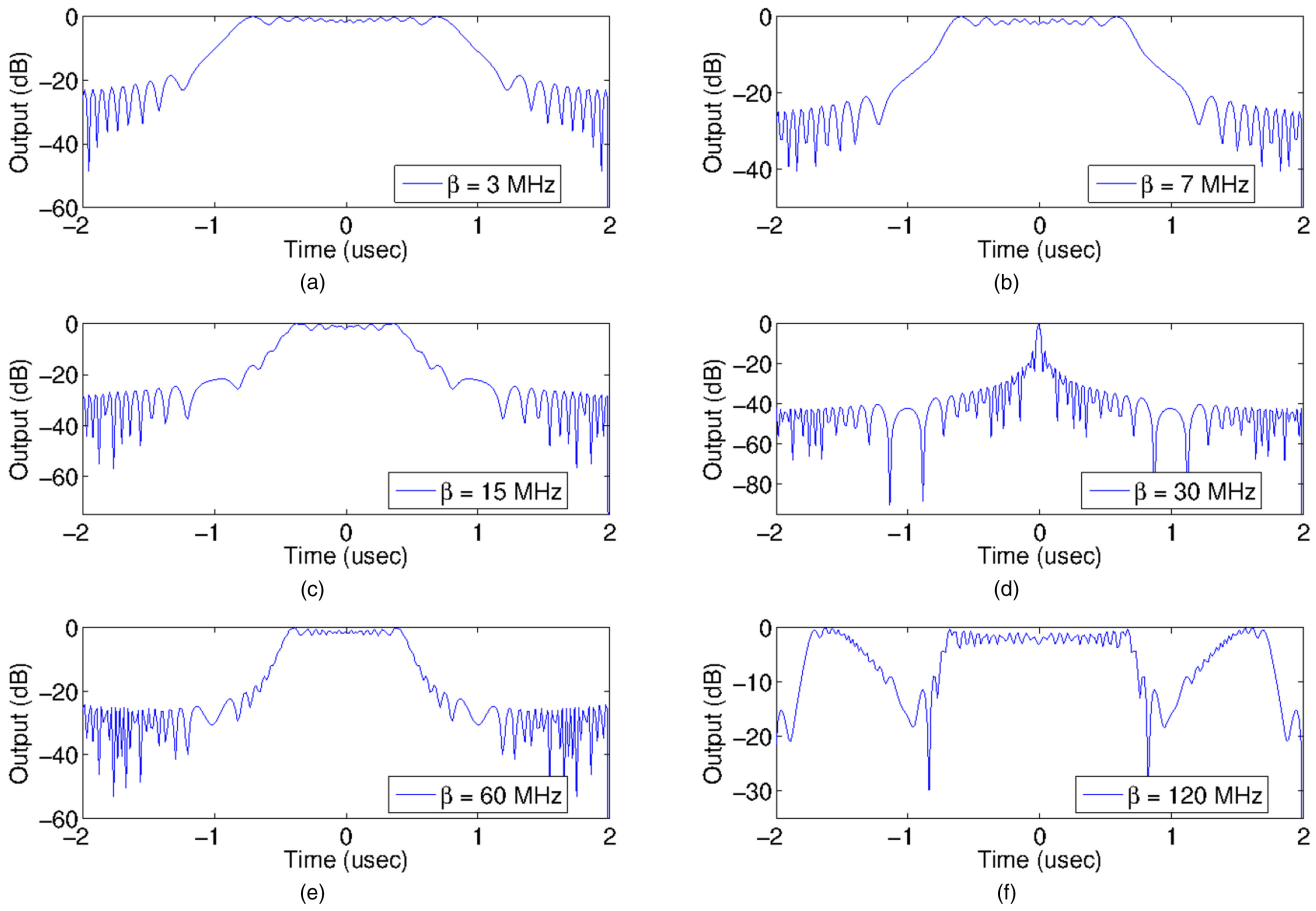

Fig. 2. Cross-correlation output of ELINT receiver for varying bandwidth from (a) $\beta = 3$ MHz, (b) $\beta = 7$ MHz, (c) $\beta = 15$ MHz, (d) $\beta = 30$ MHz, (e) $\beta = 60$ MHz, and (f) $\beta = 120$ MHz. Output of ELINT receiver, as defined in (5), successfully intercepts chirp waveform when $\beta = 30$ MHz. This outcome is equivalent to $\kappa = 0$.

intercept-receiver, defined as

$$\begin{aligned}
\tilde{y}_1[l] &= \sum_{n=-N}^{N} \tilde{s}_1[n] g^*[n-l] \\
\tilde{y}_2[l] &= \sum_{n=-N}^{N} \tilde{s}_2[n] g^*[n-l] \\
&\vdots \\
\tilde{y}_{M-1}[l] &= \sum_{n=-N}^{N} \tilde{s}_{M-1}[n] g^*[n-l] \\
\tilde{y}_M[l] &= \sum_{n=-N}^{N} \tilde{s}_M[n] g^*[n-l]
\end{aligned} \tag{5}$$

where N is the fast-time samples created by digital conversion in the intercept-receiver and l is the sampled delay relative to the ELINT intercept-receiver.

A. Chirp Waveform ($\kappa = 0$)

Figure 2 considers a chirp having bandwidth $\beta = 30$ MHz, and is the waveform being sensed by the intercept-receiver. Six different intercept-receiver outputs are evaluated and their corresponding subplots are shown in the figure. Each output incorporates a different set of parameters corresponding to different chirp replicas stored in memory by the intercept-receiver. Initially, the output of the cross-correlation process in the intercept-receiver does not produce any well-distinguished correlation peaks. Correlation at the intercept-receiver is eventually achieved when the intercept-receiver employs the chirp replica having $\beta = 30$ MHz and sweep-time 2 μs. As evidenced by the figure, a well-defined peak results for subplot (d) in the figure and suggests that the intercept-receiver successfully determines the chirp waveform characteristics. This outcome is identical to what one would expect when employing the APCN waveform for $\kappa = 0$ (not shown) since the random phase component is removed and with it, the means to mask the intercept-receiver correlation process.

B. APCN ($\kappa = 0.25 : 1$)

Figure 3 considers an APCN with bandwidth $\beta = 30$ MHz and $\kappa = 0.25$. The APCN described here is

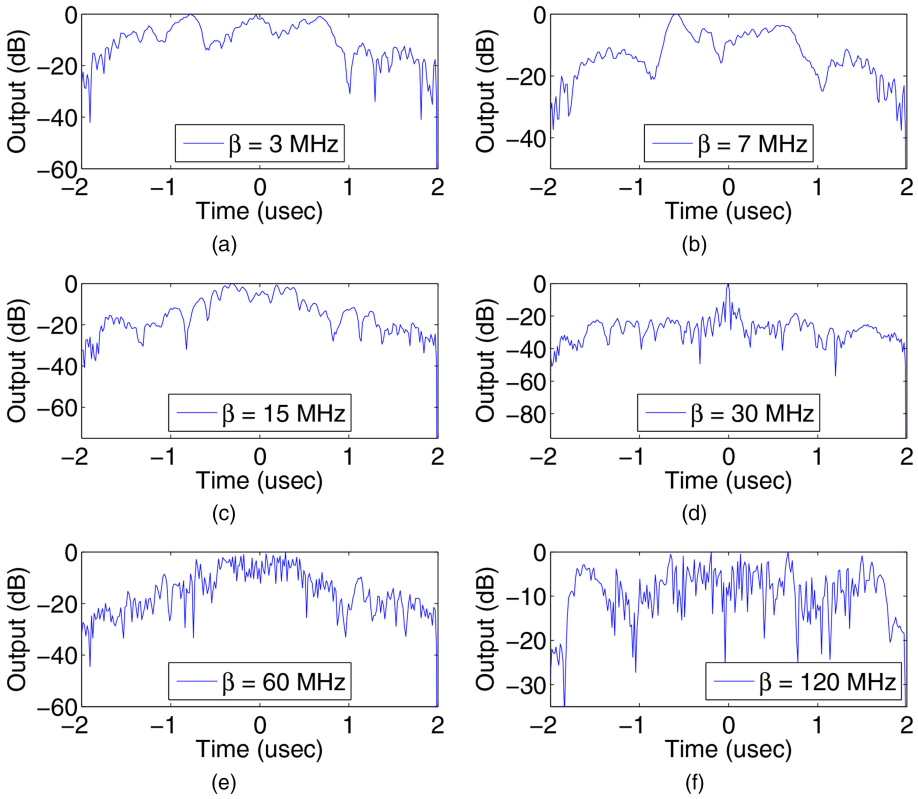

Fig. 3. Cross-correlation output of ELINT receiver for varying bandwidth from (a) $\beta = 3$ MHz, (b) $\beta = 7$ MHz, (c) $\beta = 15$ MHz, (d) $\beta = 30$ MHz, (e) $\beta = 60$ MHz, and (f) $\beta = 120$ MHz. Output of ELINT receiver, as defined in (5), successfully intercepts chirp waveform when $\beta = 30$ MHz. $\kappa = 0.25$.

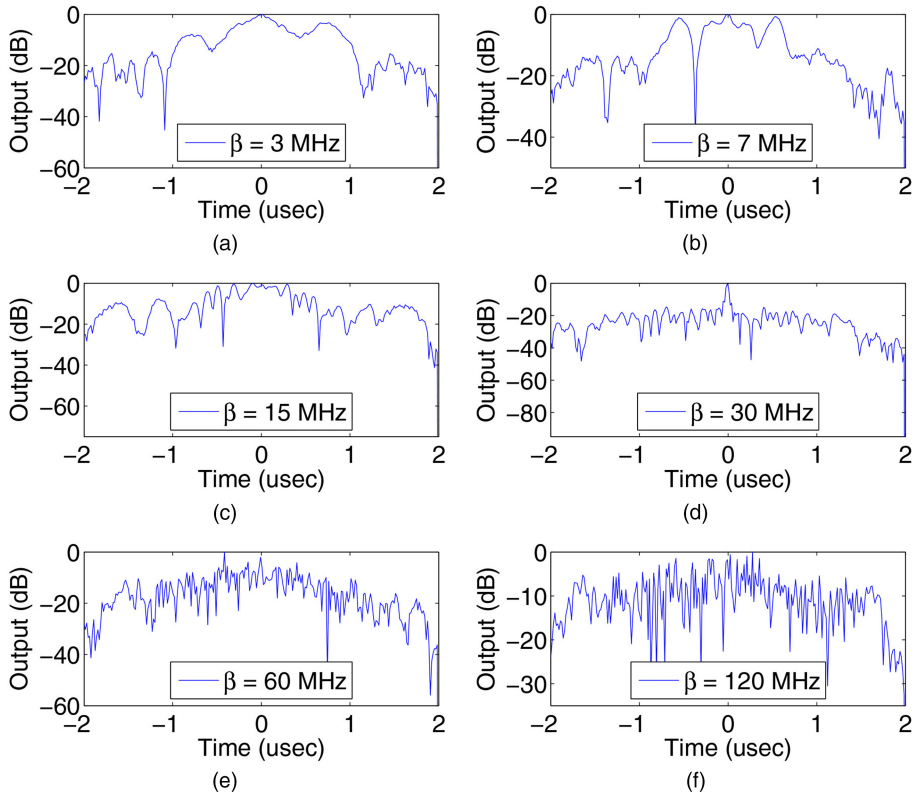

Fig. 4. Cross-correlation output of ELINT receiver for varying bandwidth from (a) $\beta = 3$ MHz, (b) $\beta = 7$ MHz, (c) $\beta = 15$ MHz, (d) $\beta = 30$ MHz, (e) $\beta = 60$ MHz, and (f) $\beta = 120$ MHz. Output of ELINT receiver, as defined in (5), successfully intercepts chirp waveform when $\beta = 30$ MHz. $\kappa = 0.5$.

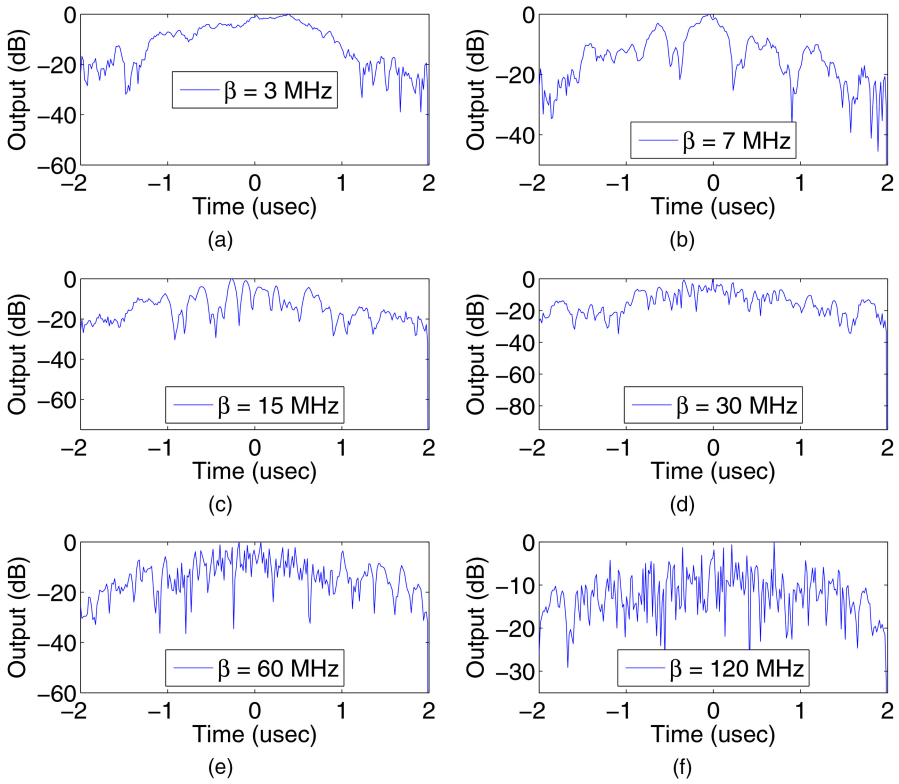

Fig. 5. Cross-correlation output of ELINT receiver for varying bandwidth from (a) $\beta = 3$ MHz, (b) $\beta = 7$ MHz, (c) $\beta = 15$ MHz, (d) $\beta = 30$ MHz, (e) $\beta = 60$ MHz, and (f) $\beta = 120$ MHz. Output of ELINT receiver, as defined in (5), is unsuccessful at correlating with APCN waveform when $\beta = 30$ MHz. $\kappa = 1$.

the waveform being sensed by the intercept-receiver. Once again, six different intercept-receiver outputs are evaluated and their corresponding subplots are shown in the figure. Initially, the output of the cross-correlation process in the intercept-receiver does not produce any well-distinguished correlation peaks. Correlation at the intercept-receiver is eventually achieved when the intercept-receiver employs the chirp replica having $\beta = 30$ MHz and sweep-time 2 μs. As evidenced by the figure, a peak results for subplot (d) in the figure and suggests that the intercept-receiver successfully determines the waveform characteristics. This correlation peak is about 8 dB weaker than the $\kappa = 0$ case as measured by their peak-to-sidelobe levels.

The APCN waveform with bandwidth $\beta = 30$ MHz and $\kappa = 0.5$ and 1 are evaluated, respectively. The APCN ($\kappa = 0.5$) case is shown in Fig. 4. As evidenced by the figure, a faint peak results for subplot (d) and suggests that the intercept-receiver could determine the waveform characteristics. This correlation peak is about 13 dB weaker than the $\kappa = 0$ case as measured by their peak-to-sidelobe levels. Traditionally, a peak-to-sidelobe ratio of 13 dB is accepted as the minimum detection threshold required at the receiver when channel noise is present. Since we did not consider any channel noise in our model, the measured sidelobe level suggests that the APCN ($\kappa = 0.5$) would challenge the intercept-receiver in a real communications channel.

The APCN ($\kappa = 1$) case is shown in Fig. 5. As evidenced by the figure, a peak does not result for subplot (d) in the figure as one would expect. The phase of the APCN ($\kappa = 1$) waveform is completely random in this case. This outcome suggests that the intercept-receiver is unsuccessful at determining the radar waveform characteristics.

IV. CONCLUSIONS

The cross-correlation output of a passive ELINT intercept-receiver designed to correlate with chirp radar waveform has been simulated. We demonstrated that a radar system employing the APCN waveform has the ability to mask its chirp-like characteristics, and in this respect, is LPI as one would expect with a random signal. We concluded that the measured sidelobe level for the APCN ($\kappa \geq 0.5$) case would challenge the intercept-receiver.

A select point not addressed in this paper pertains to the detection performance of the APCN with considerations for SNR dependencies on the nonuniform transmit power envelope. With this in mind the detection capability of the APCN waveform can be substantiated. Furthermore, future research will focus on ways to adaptively select the appropriate phase scaling factor as a function of the operational environment.

MARK A. GOVONI
U.S. Army CERDEC
Radar Division
Aberdeen Proving Ground, MD 21005

HONGBIN LI
Stevens Institute of Technology
Hoboken, NJ 07030

JOHN A. KOSINSKI
Monmouth University
W. Long Branch, NJ 07764
and
MacAulay-Brown
Dayton, OH 45430

REFERENCES

[1] Skolnik, M.
Radar Handbook.
New York: McGraw-Hill, 2008, pp. 4.1–4.6.

[2] Glenn, A.
Jamming vulnerability of communications systems.
IRE Transactions on Communications Systems, **9**, 3 (Sept. 1961), 226–232.

[3] Schleher, D. C.
Electronic Warfare in the Information Age.
Norwood, MA: Artech House, 1999.

[4] Schroer, R.
Electronic warfare.
IEEE Aerospace and Electronic Systems Magazine, **18**, 7 (July 2003), 49–54.

[5] Li, N. and Zhang, Y.
A survey of radar ECM and ECCM.
IEEE Transactions on Aerospace and Electronic Systems, **31**, 3 (July 1995), 1110–1120.

[6] Roome, S.
Digital radio frequency memory.
IEE Electronics and Communications Engineering Journal, (Aug. 1990), 147–153.

[7] Guosui, L., et al.
The present and future of random signal radars.
IEEE Aerospace and Electronic Systems Magazine, **12**, 10 (Oct. 1997), 35–40.

[8] Narayanan, R. M. and Dawood, M.
Doppler estimation using a coherent ultrawide-band random noise radar.
IEEE Transactions on Antennas and Propagation, **48**, 6 (Jan. 2000), 868–878.

[9] Sun, H., Lu, Y., and Liu, G.
Ultra-wideband technology and random signal radar: An ideal combination.
IEEE Aerospace and Electronic Systems Magazine, **18**, 11 (Nov. 2003), 3–7.

[10] Axelsson, S.
Noise radar using random phase and frequency modulation.
Proceedings of the IEEE International Geoscience and Remote Sensing Symposium, vol. 7, July 2003, pp. 4226–4231.

[11] Lukin, K. A., et al.
Implementation of software radar concept in surveillance radar on the basis of pulsed noise waveform.
Abstracts of International Conference on the Noise Radar Technology (NRT 2003), Kharkov, Ukraine, Oct. 2003, pp. 15–16.

[12] Soumekh, M.
SAR-ECCM using phase-perturbed LFM chirp signals and DRFM repeat jammer penalization.
IEEE Transactions on Aerospace and Electronic Systems, **42**, 1 (Jan. 2006), 191–205.

[13] Kalinin, V., et al.
Ultra wideband wireless communication on the base of noise technology.
Proceedings of the International Conference on Microwaves, Radar & Wireless Communications (MIKON), Krakow, Poland, May, 2006, pp. 615–618.

[14] Kulpa, K., et al.
Quality enhancement of image generated with bistatic ground-based noise waveform SAR.
IET Radar, Sonar and Navigation, **2**, 4 (2008), 263–273.

[15] Lukin, K. A., et al.
Ka-band bistatic ground-based noise waveform SAR for short range applications.
IET Radar, Sonar and Navigation, **2**, 4 (2008), 233–243.

[16] Tarchi, D., et al.
SAR imaging with noise radar.
IEEE Transactions on Aerospace and Electronic Systems, **46**, 3 (July 2010), 1214–1225.

[17] Li, Z. and Narayanan, R. M.
Doppler visibility of coherent ultrawideband random noise radar systems.
IEEE Transactions on Aerospace and Electronic Systems, **42**, 1 (Jan. 2006), 160–173.

[18] Richards, M.
Fundamentals of Radar Signal Processing.
New York: McGraw-Hill, 2005, pp. 188–198.

[19] Govoni, M. A.
Linear frequency modulation of stochastic radar waveform.
Ph.D. dissertation, Stevens Institute of Technology, Hoboken, NJ, Apr. 2011.

[20] Liu, G., et al.
The analysis and design of modern low probability of intercept radar.
Proceedings of CIE International Conference on Radar 2001, Beijing, Jan. 2001, pp. 120–124.

[21] Garmatyuk, D. and Narayanan, R. M.
ECCM capabilities of an ultrawideband bandlimited random noise imaging radar.
IEEE Transactions on Aerospace and Electronic Systems, **38**, 4 (Oct. 2002), 1243–1255.

[22] Guo, J., Li, J., and Lu, Q.
Survey on radar ECCM methods and trends in its development.
Proceedings of CIE International Conference on Radar 2006, Beijing, Oct. 2006, pp. 1–4.